neither glycoprotein IIb/IIIa inhibitors nor clopidogrel had been approved for clinical use in Japan. Beforehand, all patients received two kinds of antiplatelet agents, ticlopidine 200 mg/day (standard dose under clinical approval in Japan) and aspirin 100–200 mg/day, longer than 48 h before the PCI for the prevention of acute or subacute thrombosis. Exclusion criteria were (i) acute myocardial infarction within 48 h from onset ($n = 3$), (ii) restenotic lesions after balloon angioplasty or ISR ($n = 7$), (iii) a low ejection fraction of the left ventricle ($n = 2$), (iv) left main disease or ostial lesions ($n = 12$), and (v) tortuous vessels or heavily calcified vessels proximal to the culprit lesions ($n = 8$) because of the expected difficulty in acquiring angioscopic images for the whole stented segments or in advancing the angioscopic catheter. Finally, 21 patients were enrolled in the SES group. Between October 2000 and May 2001, 61 patients were treated with BMSs. According to the above exclusion criteria, 36 patients (20 acute myocardial infarction, five restenosis, three low ejection fraction, four ostial lesions, and four vessel tortuousity or calcification) were excluded. Consequently, 25 patients were selected as the BMS group. All patients included this study received follow-up angiography and angioscopy at 6 months. Written informed consent approved by our institutional review board was obtained from all study patients before catheterization.

Clinical demographics

The patient demographics were obtained by a hospital chart review. Stable angina pectoris (SAP) was defined as a positive stress test and no change in the frequency, duration, or intensity of symptoms within 4 weeks. Unstable angina was new-onset severe angina, accelerated angina, or rest angina. Recent myocardial infarction was defined as its occurrence between 2 days and 2 weeks before the PCI. Patients with acute myocardial infarction less than 2 days from onset were not enrolled. Patients with unstable angina and recent myocardial infarction were categorized as acute coronary syndrome (ACS).

Culprit lesions (target lesions of the PCI) were identified by a combination of the ECG findings, wall motion abnormalities on left ventriculography or the echocardiography findings, and angiographic lesion morphology.

Angiographic analysis

All angiograms were analysed with a computer-assisted, automated edge detection algorithm (CMS, MEDIS, Nuenen, The Netherlands) by an angiographer blinded to the clinical and angioscopic findings using standard qualitative definition and quantitative coronary angiogram measurements. A 6-month follow-up angiogram was performed at the same angle as the PCI. The reference vessel diameter (RVD), minimal lumen diameter (MLD), per cent diameter stenosis (%DS), lesion length, and late loss at the culprit lesion or stented segment were measured. Angiographic filling defects, haziness, or wall irregularity was qualitatively evaluated. ISR was defined as more than or $\geq$50% of DS at follow-up, located within the stented segments and in the segments adjacent to the proximal and distal edge of the stent.

Coronary angioscopic imaging

The coronary angioscopic procedure has been previously reported.[12] Angioscopic examinations were performed before PCI, immediately after PCI, and 6 months after PCI as follow-up studies. Culprit plaques and whole-stented segments were observed with an angioscopic catheter (Vecmova Neo, Clinical Supply Corp., Gifu, Japan). The angioscopic images and fluoroscopy during the angioscopic observations were recorded on digital videotape for later analysis. The exact position of the angioscopic catheter at the observed segment was recorded by an angiogram to ensure a reliable comparison.

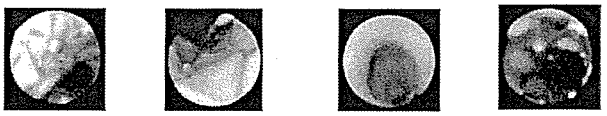

Figure 1 Angioscopic images of the neointimal stent coverage grade at follow-up and thrombus. (*A*) Stent coverage grade 0. No neointima was found on the struts of two overlapping SESs. The struts seemed to be completely exposed to the lumen. (*B*) Stent coverage grade 1. The struts were seen under the thin neointima. (*C*) Stent coverage grade 2. The struts were fully covered by white neointima and could not be seen. (*D*) Red thrombus was found around the struts (between 11 and 1 o'clock).

Definition and analysis of angioscopic findings

The plaque colour, the existence of a plaque rupture, and the existence of thrombus on the culprit plaque were evaluated before PCI. On the basis of the surface colour of the culprit plaque, the yellow grade was classified as 0 (white), 1 (light yellow), 2 (yellow), or 3 (dark yellow) according to the criteria established in our previous report.[13] A plaque rupture was defined as a complex plaque, which was considered to be present when the surface of the lesion had an irregular appearance, including a fissure, flap, and ulceration. A thrombus was defined a coalescent red or a pinkish-white, superficial or protruding mass adhering to the vessel surface but clearly a separate structure that remained, despite being flushed with a saline solution (*Figure 1*). Immediately after the PCI, both the plaque colour and the existence of thrombus within the stented segments were observed by repeat angioscopic examinations for a complete assessment of their angioscopic items. Six months after the PCI, the plaque colour, the existence of thrombus, and stent coverage by neointimal hyperplasia were all evaluated. The yellow grade regression was defined as the yellow grade immediately after stenting minus that at the 6-month follow-up. The extent of neointimal stent coverage was evaluated using a semi-quantitative grading system: 0, absent neointimal coverage by macroscopic detection; 1, visible struts through thin neointima; and 2, completely buried struts under the neointima (invisible struts through the neointima) (*Figure 1*). The neointimal stent coverage was estimated at major three different parts of the stented segment such as the edge the body, and the overlapping segment. Stent struts located at the orifice of the side branches were excluded from this evaluation. The minimum coverage grade at each segment was selected as the stent coverage grade.

The intra-observer agreement on angioscopic images was measured by having an observer repeat assessment of 20 images (presented in random order) after 1 week. The inter-observer agreement was measured by comparing the assessment of 50 images by the two observers blinded to the clinical background. The intra-observer agreements for the evaluated angioscopic items were 95% in existence of plaque rupture, 95% in yellow grade of the plaque, 100% in existence of thrombus, and 95% in stent coverage grade. The inter-observer agreements of those items were 92, 90, 96, and 90%, respectively.

Clinical follow-up

Two kinds of antiplatelet agents, ticlopidine (200 mg/day) added to aspirin (100–200 mg/day), were administered continuously during the 6-month follow-up period. Repeat PCI, coronary bypass surgery, the occurrence of ACS, and cardiac sudden death were all considered to be major adverse events.

Statistical analysis

The statistical analysis was performed using StatView 5.0 (SAS Institute). Categorical variables are presented as frequencies and

Table 1 Patients' characteristics

Patients	SES ($n = 21$)	BMS ($n = 25$)	*P*-value
Age (years)	66 ± 7	62 ± 11	0.12
Gender (male)	19 (90%)	20 (87%)	0.71
Coronary risk factors			
Diabetes mellitus	8 (38%)	6 (26%)	0.39
Hypertension	9 (43%)	12 (52%)	0.54
Hyperlipidaemia	14 (67%)	18 (78%)	0.39
Current smoking	8 (38%)	11 (48%)	0.52
Body mass index (kg/m^2)	24 ± 3	25 ± 4	0.36
Diagnosis of coronary artery disease			
SAP	16 (76%)	18 (78%)	0.87
ACS	5 (24%)	5 (22%)	
Prior myocardial infarction	9 (43%)	7 (30%)	0.39
Prior PCI	6 (29%)	5 (22%)	0.60
Prior bypass surgery	0 (0%)	0 (0%)	>0.99
Multi-vessel disease	10 (48%)	10 (43%)	0.78
Medications			
ACE-inhibitor or ARB	13 (62%)	12 (52%)	0.52
Beta-blocker	8 (38%)	12 (52%)	0.26
Calcium antagonist	5 (24%)	8 (35%)	0.43
Statin	17 (81%)	20 (87%)	0.59
Warfarin	1 (5%)	0 (0%)	0.48
Insulin	1 (5%)	1 (4%)	0.95
Oral hypoglycaemic agents	6 (29%)	5 (22%)	0.60

Values are *n* (%) or the mean ± SD. ACE, angiotensin-converting enzyme; ARB, angiotensin II receptor blocker.

they were analysed by either the χ^2 test or the Fisher's exact test. Continuous quantitative data and discontinuous data (angioscopic grades for plaque colour and stent coverage) are presented as mean ± SD. Continuous data were compared by the unpaired Student's *t*-test between the different categories. Ordinal data of stent coverage grade were tested by the Mann–Whitney *U* test with the Bonferroni's correction between the different categories (between different segments in the same kind of stent and corresponding segment between different kinds of stents). The yellow grade among the same categories between those observed at baseline and at follow-up was compared by the Wilcoxon singed-rank test with the Bonferroni's correction. A *P*-value of <0.05 was considered to be statistically significant.

Results

Clinical characteristics at baseline

Thirty-three SESs were implanted in 21 lesions of 21 patients and 33 BMSs were implanted in 28 lesions of 25 patients. The patients' characteristics in the SES group ($n = 21$) and those in the BMS group ($n = 25$) at baseline are summarized in *Table 1*. No significant difference in the age, proportion of gender, risk factors of atherosclerosis, including diabetes mellitus, diagnosis for coronary artery disease (SAP or ACS), or medications, existed between the two groups.

Angiographic findings

The angiographic data are summarized in *Table 2*. The lesion location did not differ between the two groups. Before PCI, RVD was greater in the BMS group than that in the SES group and the lesion length was longer in the SES group than that in the BMS group. The frequency of filling defects or haziness did not differ between the two groups. Immediately after PCI, both of MLD and acute gain were greater in the BMS group than that in the SES group. At the 6-month follow-up, both the %DS and late loss were smaller in the SES group than that in the BMS group. There were no filling defects, haziness, or wall irregularity in neither of the two groups at follow-up. Despite the fact that one case in the SES group showed focal ISR, no edge restenosis was seen on the angiogram. The SES group tended to show a decreased ISR rate in comparison to the SES group (5 vs. 24%, $P = 0.07$).

Table 2 Angiographic findings

Patients	SES ($n = 21$)	BMS ($n = 25$)	*P*-value
Lesion location			
LAD	14 (67%)	17 (68%)	0.92
LCx	5 (24%)	4 (16%)	0.51
RCA	2 (9%)	7 (28%)	0.12
Before PCI			
RVD (mm)	2.81 ± 0.24	3.14 ± 0.32	0.0003
MLD (mm)	0.58 ± 0.31	0.59 ± 0.18	0.008
%DS	69.8 ± 13.8	71.0 ± 10.1	0.013
Lesion length (mm)	22.9 ± 10.8	13.0 ± 4.95	0.0002
Filling defects, haziness, or wall irregularity	4 (19%)	5 (20%)	0.94
Immediately after PCI			
MLD (mm)	2.64 ± 0.23	2.95 ± 0.25	0.00008
%DS	11.7 ± 2.97	12.8 ± 4.46	0.34
Acute gain (mm)	2.06 ± 0.32	2.36 ± 0.27	0.0013
Filling defects, haziness, or wall irregularity	2 (10%)	1 (4%)	0.45
Six-month follow-up			
MLD (mm)	2.55 ± 0.33	2.45 ± 0.65	0.53
%DS	14.0 ± 6.31	30.1 ± 15.1	0.00004
Late loss (mm)	0.09 ± 0.25	0.50 ± 0.57	0.0038
ISR	1 (5%)	6 (24%)	0.07
Filling defects, haziness, or wall irregularity	0 (0%)	0 (0%)	>0.99

Values are *n* (%) or the mean ± SD. LAD, left anterior descending artery; LCx, left circumflex artery; RCA, right coronary artery.

Angioscopic findings

Angioscopic findings at baseline (before and immediately after PCI) and at the 6-month follow-up are summarized in *Table 3*. Before PCI, the frequency of plaque rupture and yellow grade of the culprit plaque did not differ between the two groups. At baseline, thrombus was observed in seven lesions (five in ACS and two in SAP) of seven SES patients and in seven lesions of seven BMS patients (five in ACS and two in SAP), and the frequency of the thrombus was similar between the two groups (33 vs. 28%, respectively). At the 6-month follow-up, the yellow grade of the culprit plaque was higher in the SES group than that in the BMS group (1.1 ± 0.5 vs. 0.5 ± 0.6, $P = 0.0007$). The relatioship between the yellow grade regression and the frequency of the patients is presented in *Figure 2*.

Table 3 Angioscopic findings at baseline and follow-up

Patients	SES ($n = 21$)	BMS ($n = 25$)	*P*-value
Baseline			
Plaque rupture (Before PCI)	4 (19%)	5 (20%)	0.94
Yellow grade of the culprit plaque	1.4 ± 0.6	1.6 ± 0.9	0.39
Thrombus	7 (33%)	7 (28%)	0.022
Six-month follow-up			
Yellow grade of the culprit plaque	1.1 ± 0.5	0.5 ± 0.6	0.0007
Thrombus	7 (33%)	2 (8%)	0.049

Values are *n* (%) or mean ± SD.

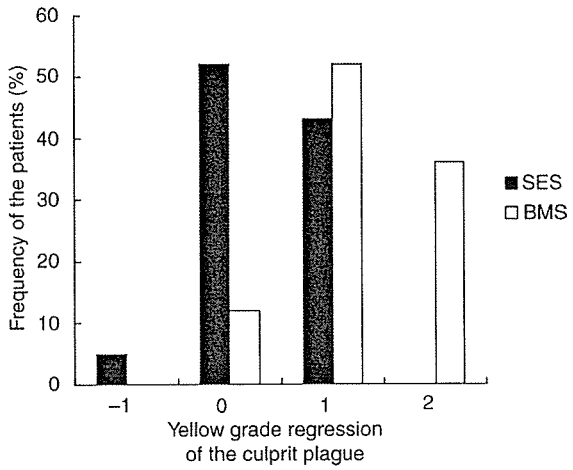

Figure 2 The relationship between the yellow grade regression of the culprit plaque and the frequency of the patients. In the SES group, the yellow grade regression of −1, 0, 1, and 2 were accounted for 5, 52, 43, and 0% of the patients, respectively. In the BMS group, that of −1, 0, 1, and 2 were accounted for 0, 12, 52, and 36% of the patients, respectively.

The yellow grade regression of the culprit plaque was lower in the SES group than that in the BMS group (0.3 ± 0.6 vs. 1.1 ± 0.7, $P < 0.0001$). In the SES group, six of seven thrombi found at baseline remained at the 6-month follow-up, and one thrombus was newly recognized at follow-up. As a result, seven thrombi in the SES group were observed at follow-up. In the BMS group, two of seven thrombi found at baseline remained at the 6-month follow-up, and there was no thrombus formation during the 6-month follow-up period. The frequency of persistence of thrombus was higher in the SES group than that in the BMS group (86 vs. 29%, respectively; $P = 0.031$) (*Figure 3*). The angioscopic and angiographic findings for each case in the SES and the BMS groups are shown in *Figure 4*.

In the SES group, a single SES was deployed in 11 lesions, two SESs were placed in eight lesions, and three SESs were used in two lesions. In the BMS group, a single BMS was deployed in 23 lesions and two BMSs were placed in five lesions. In both of the groups, multiple stent deployment for a single lesion completely overlapped without a gap. At the 6-month follow-up, 21 stent edges, 33 stent bodies, and the 12 stent overlapping segments of the SES group

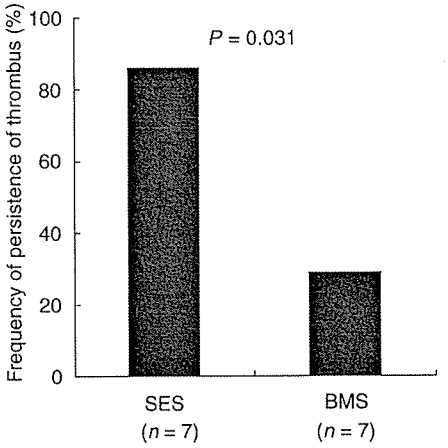

Figure 3 A comparison of the frequency of persistence of thrombus between the SES and BMS. The frequency of persistence of thrombus was significantly higher in the SES than in the BMS (86 vs. 29%, respectively).

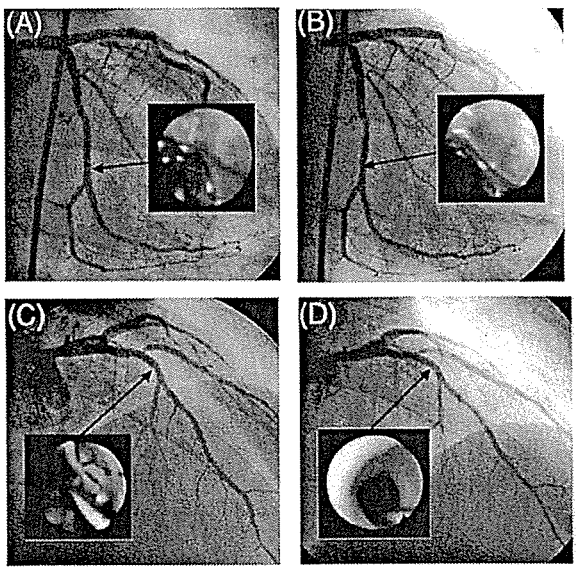

Figure 4 Two cases showing the angiographic and angioscopic findings after stent implantation in thrombotic lesions. (*A*) Immediately after SES implantation in the left circumflex artery in a patient with ACS. A pinkish mural thrombus was clearly found (between 0 and 5 o'clock) beside the plaque of the yellow grade 3 (at 11 o'clock). (*B*) A follow-up exam at 6 months in the case shown in (*A*). ISR was not seen on the angiogram. Residual thrombus was recognized (between 0 and 2 o'clock). Parts of the struts were absent in the neointimal coverage (the stent coverage grade 0), and a thin neointimal proliferation on the plaque of the yellow grade 2 (between 2 and 4 o'clock) was found. The yellow grade regression was 1 in this case. (*C*) Immediately after BMS implantation in the left anterior descending artery in a patient with ACS. A pinkish mural thrombus was found (between 0 and 8 o'clock) beside the plaque of the yellow grade 2 (between 0 and 3 o'clock). (*D*) A follow-up exam at 6 months in the case shown in (C). ISR was not seen on the angiogram. There was no residual thrombus. The struts were completely covered by neointima (the stent coverage grade 2 and the yellow grade 0). The yellow grade regression was 2 in this case.

were analysed for the stent coverage grade. Similarly, 28 stent edges, 33 stent bodies, and five stent overlapping segments of the BMS group were analysed. In all segments, the stent coverage grade for the SES was lower than that for the BMS (1.1 ± 0.7 vs. 1.9 ± 0.4, respectively; $P < 0.0001$).

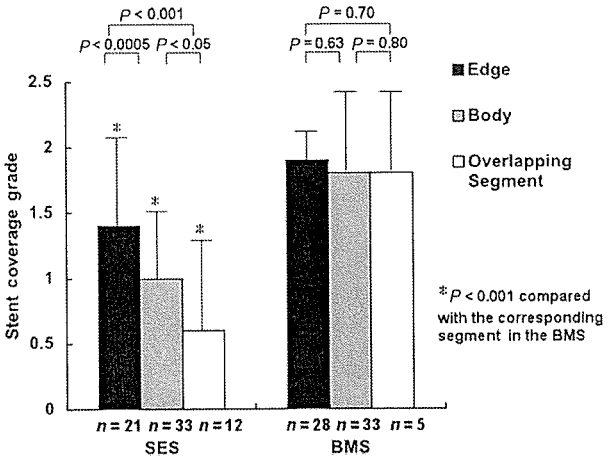

Figure 5 A comparison of the stent coverage grade in different stent segments between the SES and the BMS. The stent coverage grade in the SES was lower in the body than in the edge and in the overlapping segment than in the body. The coverage grade in the BMS did not differ between the edge, body, or the overlapping segment. This grade of the SES was lower than that of the BMS in every different segment.

The stent coverage grade in the SES was 1.4 ± 0.7 in edge, 1.0 ± 0.5 in body, and 0.6 ± 0.7 in overlapping segment. This grade was lower in the body than in the edge ($P = 0.0002$) and in the overlapping segment than in the body ($P = 0.016$). In the BMS group, the stent coverage grade in the edge body and overlapping segment was 1.9 ± 0.2, 1.8 ± 0.5, and 1.8 ± 0.5, respectively. No segment was significantly different from another. The stent coverage grade of the SES group was lower than that of the BMS group, in the edge ($P < 0.0001$), the body ($P < 0.0001$), and the overlapping segment ($P = 0.0069$) (*Figure 5*). A total of 27 segments (41% of all segments; six edges, 15 bodies, and six overlapping segments) of the SES and four segments (6% of all segments; four bodies) of the BMS were evaluated to have an absence of neointimal coverage (grade 0).

Clinical events

All patients underwent successful PCI for culprit lesions at baseline. Four lesions in three patients (12%) in the BMS group and none of the patients in the SES group underwent repeat PCI for ISR 6 months after the first PCI. All patients in both groups were free from bypass surgery, ACS, and cardiac sudden death during the clinical follow-up period.

Discussion

Although several follow-up studies after SES implantation revealed the effect of neointimal proliferation on its inhibition, there is a lack of detailed data regarding changes in underlying atherosclerotic yellow plaque due to neointimal stent coverage and intracoronary thrombus. Coronary angioscopy provides detailed information on plaque colour, neointimal hyperplasia, and mural thrombus by the direct visualization of the coronary lumen. Our angioscopic follow-up study demonstrated that the processes of changes in yellow plaque, neointimal coverage, and thrombus disappearance within the stented segments in the SES occurred more slowly than those in the BMS.

Differences in neointimal coverage between SES and BMS

The grade of neointimal coverage after BMS implantation was previously classified as either 0: complete exposure of stent struts, 1: exposure of the struts with partial coverage, 2: more than 50% coverage, 3: almost complete coverage with slightly visible the struts, or 4: complete coverage.[12] However, it was difficult to determine this grade from 1 to 3 after SES implantation, because neointimal growth over the SES was frequently too thin and was partially transparent. The transparent neointima diagnosed by angioscopy may be layer of fibrin deposition.[16] Therefore, simple grading system of the neointimal coverage was used in this study.

Experimental models of rabbit's iliac arteries confirmed that SES shows a decrease in neointimal thickness of 26.3% in comparison to BMSs (Bx velocity stents), platform of the SES.[16] At the 6-month follow-up, the late loss on the angiogram in the SES was smaller than that in the BMS. The stent coverage grade on the angioscopic findings in the overall stented segments in the SES was lower than that in the BMS. These results thus supported the notion that the neointimal proliferation inside the SES at the chronic phase was inhibited to be thinner than that in the BMS, and this finding was similar to the findings of previous IVUS investigations in living patients.[4,5,7,8]

One of the major factors that influence angioscopic yellow grade is thickness of the fibrous cap or neointima over atherosclerotic lipid contents. Thick neointimal hyperplasia after stenting might change the plaque colour from yellow to white or reduce the yellow grade. Therefore, the differences in the yellow grade regression of the culprit plaque between the SES and the BMS may be explained by the differences in the thickness of the neointimal hyperplasia. The thin neointima over the SES struts on the yellow plaque may make it easier to find the struts through the neointima and it may also be less influential in changing the yellow grade of the plaque.

Differences in neointimal coverage between the different segments

Angioscopic neointimal coverage over the BMS at the 6-month follow-up was almost complete and equal on the edge, in the body, and in the overlapping segment of the stents. In contrast, the degree of neointimal coverage of the SES differed between the edge, the body, and the overlapping segment. The neointimal coverage grade of the SES was significantly lower in the overlapping segment than in the body. These angioscopic results agree with the findings of a recent pathohistological report by Finn *et al.*[16] in which they demonstrated that both incomplete endothelialization (delayed endothelialization) as assessed by light microscopy and chronic inflammation were found more commonly in the overlapping segments than in the non-overlapping segments of the SES.[16] They speculated that the poor endothelialization and persistent inflammation in the overlapping segment are based on the contribution of drug overdose, a hypersensitive reaction to the polymer, and/or metal overload. In the present study, 27 of 66 segments (41%) of the SES were evaluated to have an absence of neointimal coverage and an exposure of the struts on angioscopy. A macroscopic diagnosis using

angioscopy has limitation to detect infiltration of inflammatory cells, tiny fibrin deposition, and very thin neointimal proliferation on the struts.[17] Other imaging modalities with a high-resolution, such as optical coherence tomography, may help to clarify the fine structure inside the SES.[17]

Previous IVUS studies revealed that the SES does not create any of the edge effects predominantly caused by negative remodelling with exaggerated neointimal hyperplasia.[5,7,8] In the present study, angioscopic neointimal coverage grade of the SES was higher in the edge than in the body at follow-up. The precise mechanism of the differences in the degree of neointimal proliferation is not clear. Several speculative hypotheses may be raised to explain this phenomenon. First, at the proximal or distal edges, the drug dose and/or metal dose of the SES is theoretically half of that in the body because the existence of the struts is only on one side, namely either the distal or the proximal side. Secondly, the edges of the SES are usually located in non-stenotic healthy segments, whereas its bodies are in the stenotic diseased segments on the angiogram. Therefore, the composition of the vessel wall (plaque) might differ between the two locations. These differences in the composition of vessel wall (plaque) may be the cause of the differences in the degree of neointimal proliferation on angioscopy.

Differences in thrombus disappearance between SES and BMS

After stent implantation, it has been understood that smooth muscle cells in the media proliferate and migrate to the lumen surface under the influence of growth factors.[18] However, the processes of thrombus disappearance after stenting in living patients are necessarily less detailed. The neointimal growth involved in the thrombus change to fewer cellular elements and a richer extracellular matrix probably occurs over a period of weeks or months.

In our series, the SES showed more unfavourable effects on the thrombus disappearance within the stented segments than the BMS. Several possible explanations can be offered for these results. First of all, sirolimus directly inhibits the proliferation of smooth muscle cells. As a result, thrombus disappearance may be indirectly delayed due to a suppression of neointimal growth. Secondly, the *in vitro* findings indicated that sirolimus (rapamycin) by itself increases basal tissue factor levels by 40% in human aortic endothelial cells.[19] The tissue factor, contained in human atherosclerotic plaques, is well known to be one of the thrombogenic agents. The tissue factor expressed on the endothelium may therefore disturb the thrombus disappearance.

Although angioscopy has limitations to confirm the existence of very thin neointima, macroscopic examinations at the 6-month follow-up failed to reveal a complete neointimal coverage overlying the struts, especially in the overlapping segment of the SES. Moreover, most of the intracoronary thrombi within the SES remained at follow-up. It may thus be necessary to investigate the duration of aggressive antiplatelet therapy after SES implantation. In the BMS, the phenomenon that the neointima becomes thick and non-transparent until 6 months after stent implantation and then thin and transparent by 3 years has been previously reported.[20] Further long-term follow-up studies to elucidate changes in the neointima and the residual thrombi are thus required.

Study limitations

Our findings were based on observations in a relatively small number of patients and stented segments excluding acute myocardial infarction within 48 h from onset. Some selection bias is therefore inevitable. This study was not a randomized study. Therefore, the RVD before the PCI was larger in the BMS group than in the SES group. The patient characteristics between the two groups were well matched. However, under these conditions, the antiproliferative effects of the SES were demonstrated by angioscopy.

Conclusions

This study failed to prove complete neointimal coverage of SES 6 months after implantation, despite macroscopic diagnosis by angioscopy. Our angioscopic study suggested both a delayed neointimal proliferation and a slow process in thrombus disappearance in the SES in comparison with those in the BMS at 6 months after their implantation. Further long-term follow-up studies to clarify the serial changes of the neointima and thrombi inside the SES are thus called for.

Acknowledgement

This study was supported in part by the Eisai Corporation.

Conflict of interest: none declared.

References

1. Kornowski R, Hong MK, Tio FO, Bramwell O, Wu H, Leon MB. In-stent restenosis: contributions of inflammatory responses and arterial injury to neointimal hyperplasia. *J Am Coll Cardiol* 1998;31:224–230.
2. Marx SO, Marks AR. Bench to bedside: the development of rapamycin and its application to stent restenosis. *Circulation* 2001;104:852–855.
3. Suzuki T, Kopia G, Hayashi S, Bailey LR, Llanos G, Wilensky R, Klugherz BD, Papandreou G, Narayan P, Leon MB, Yeung AC, Tio F, Tsao PS, Falotico R, Carter AJ. Stent-based delivery of sirolimus reduces neointimal formation in a porcine coronary model. *Circulation* 2001;104:1188–1193.
4. Sousa JE, Costa MA, Abizaid A, Abizaid AS, Feres F, Pinto IM, Seixas AC, Staico R, Mattos LA, Sousa AG, Falotico R, Jaeger J, Popma JJ, Serruys PW. Lack of neointimal proliferation after implantation of sirolimus-coated stents in human coronary arteries: a quantitative coronary angiography and three-dimensional intravascular ultrasound study. *Circulation* 2001;103:192–195.
5. Rensing BJ, Vos J, Smits PC, Foley DP, van den Brand MJ, van den Gissen WJ, de Feijter PJ, Serruys PW. Coronary restenosis elimination with a sirolimus eluting stent: first European human experience with 6-month angiographic and intravascular ultrasonic follow-up. *Eur Heart J* 2001; 22:2125–2130.
6. Morice MC, Serruys PW, Sousa JE, Fajadet J, Ban Hayashi E, Perin M, Colombo A, Schuler G, Barragan P, Guagliumi G, Molnar F, Falotico R, RAVEL Study Group. A randomized comparison of a sirolimus-eluting stent with a standard stent for coronary revascularization. *N Engl J Med* 2002;346:1773–1780.
7. Serruys PW, Degertekin M, Tanabe K, Abizaid A, Sousa JE, Colombo A, Guagliumi G, Wijns W, Lindeboom WK, Lighthart J, de Feyter PJ, Morice MC, RAVEL Study Group. Intravascular ultrasound findings in the multicenter, randomized, double-blind RAVEL (Randomized study with the sirolimus-eluting Velocity balloon-expandable stent in the treatment of patients with de novo native coronary artery Lesions) trial. *Circulation* 2002;106:798–803.

8. Degertekin M, Lemos PA, Lee CH, Tanabe K, Sousa JE, Abizaid A, Regar E, Sianos G, van der Giessen WJ, de Feyter PJ, Wuelfert E, Popma JJ, Serruys PW. Intravascular ultrasound evaluation after sirolimus eluting stent implantation for de novo and in-stent restenosis lesions. *Eur Heart J* 2004;**25**:32–38.
9. Sousa JE, Costa MA, Abizaid A, Feres F, Seixas AC, Tanajura LF, Mattos LA, Falotico R, Jaeger J, Popma JJ, Serruys PW. Four-year angiographic and intravascular ultrasound follow-up of patients treated with sirolimus-eluting stents. *Circulation* 2005;**111**:2326–2329.
10. McFadden EP, Stabile E, Regar E, Cheneau E, Ong AT, Kinnaird T, Suddath WO, Weissman NJ, Torguson R, Kent KM, Pichard AD, Satler LF, Waksman R, Serruys PW. Late thrombosis in drug-eluting coronary stents after discontinuation of antiplatelet therapy. *Lancet* 2004;**364**:1519–1521.
11. Takano M, Mizuno K. Late coronary thrombosis in a sirolimus-eluting stent due to the lack of neointimal coverage. *Eur Heart J* 2006;**27**:1133.
12. Sakai S, Mizuno K, Yokoyama S, Tanabe J, Shinada T, Seimiya K, Takano M, Ohba T, Tomimura M, Uemura R, Imaizumi T. Morphologic changes in infarct-related plaque after coronary stent placement: a serial angioscopy study. *J Am Coll Cardiol* 2003;**42**:1558–1565.
13. Takano M, Mizuno K, Yokoyama S, Seimiya K, Ishibashi F, Okamatsu K, Uemura R. Changes in coronary plaque color and morphology by lipid-lowering therapy with atorvastatin: serial evaluation by coronary angioscopy. *J Am Coll Cardiol* 2003;**42**:680–686.
14. Okamatsu K, Takano M, Sakai S, Ishibashi F, Uemura R, Takano T, Mizuno K. Elevated troponin T levels and lesion characteristics in non-ST-elevation acute coronary syndromes. *Circulation* 2004;**109**:465–470.
15. Takano M, Inami S, Ishibashi F, Okamatsu K, Seimiya K, Ohba T, Sakai S, Mizuno K. Angioscopic follow-up study of coronary ruptured plaques in nonculprit lesions. *J Am Coll Cardiol* 2005;**45**:652–658.
16. Finn AV, Kolodgie FD, Harnek J, Guerrero LJ, Acampado E, Tefera K, Skorija K, Weber DK, Gold HK, Virmani R. Differential response of delayed healing and persistent inflammation at sites of overlapping sirolimus- or paclitaxel-eluting stents. *Circulation* 2005;**112**:270–278.
17. Takano M, Jang IK, Mizuno K. Neointimal proliferation around malapposed struts of a sirolimus-eluting stent: optical coherence tomography findings. *Eur Heart J* 2006;**27**:1763.
18. Welt FGP, Rogers C. Inflammation in the stent era. *Atheroscler Thromb Vasc Biol* 2002;**22**:1769–1776.
19. Steffel J, Latini RA, Akhmedov A, Zimmermann D, Zimmerling P, Luscher TF, Tanner FC. Rapamycin, but not FK-506, increases endothelial tissue factor expression. *Circulation* 2005;**112**:2002–2011.
20. Asakura M, Ueda Y, Nanto S, Hirayama A, Adachi T, Kitakaze M, Hori M, Kodama K. Remodeling of in-stent neointima, which become thinner and transparent over 3 years: serial angiographic and angioscopic follow-up. *Circulation* 1998;**97**:2003–2006.

Clinical vignette

doi:10.1093/eurheartj/ehi789

Huge right coronary artery aneurysm in a young adult

Kuan-Ming Chiu[1], Tzu-Yu Lin[2], and Ming-Jiuh Wang[3]*

[1]Department of Cardiovascular Surgery, Far Eastern Memorial Hospital, 21, Sec. 2, Nan-Ya South Road, Pan Chiao, Taipei 220, Taiwan; [2]Department of Anesthesia, Far Eastern Memorial Hospital, 21, Sec. 2, Nan-Ya South Road, Pan Chiao, Taipei 220, Taiwan; [3]Department of Anesthesiology, National Taiwan University Hospital and National Taiwan University College of Medicine, 7, Chung Shan South Road, Taipei 100, Taiwan

* Corresponding author. Tel: +886 2 23562010; fax: +886 2 23217522. *E-mail address*: canon@ha.mc.ntu.edu.tw

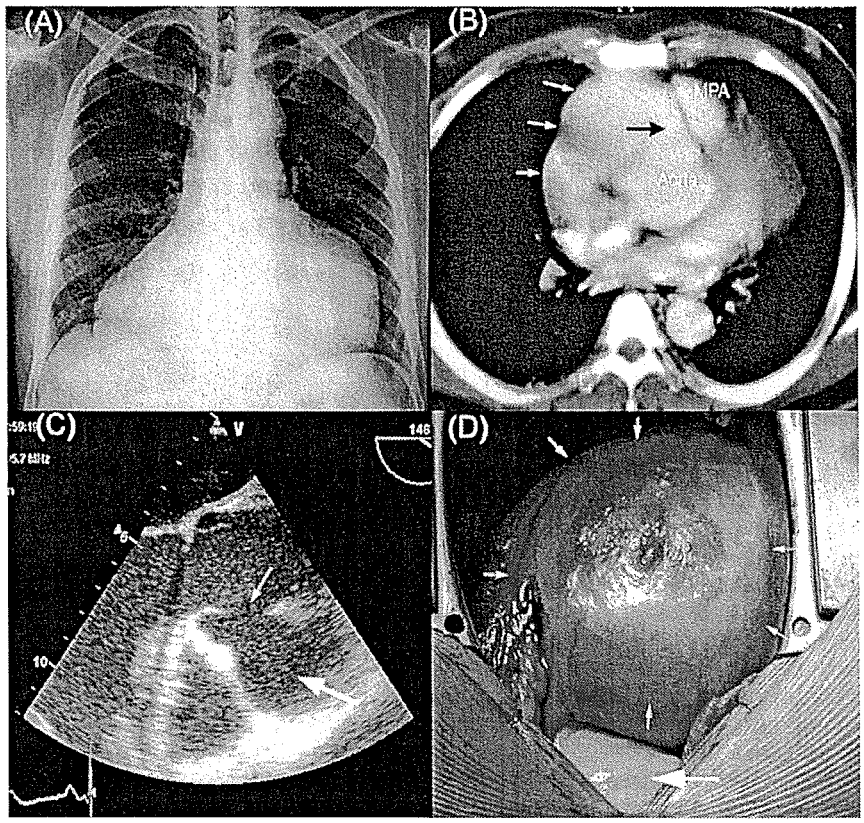

A 34-year-old man visited our institution for an abnormal chest radiograph with greatly enlarged cardiac silhouette (Panel A) found before his wedding. Detailed medical history revealed a febrile episode and a strawberry-like tongue and some 'flu-like symptoms' for >1 week when he was 5 years old. Diagnostic workup including computerized tomography demonstrated a huge right coronary artery aneurysm (Panel B). Intra-operative transesophageal echocardiography showed a large orifice of right coronary artery with a huge aneurysm (Panel C). The right coronary artery aneurysm was resected (Panel D) under hypothermic cardiopulmonary bypass with cardioplegic arrest. The diameter of the orifice of the right coronary artery was >20 mm, which was closed with Dacron patch, and the saphenous vein was used to bypass the right coronary artery to its two major branches. The patient had an uneventful recovery and was discharged 6 days after the operation.

Panel A. Chest X-ray shows an enlarged cardiac silhouette.

Panel B. Thorax CT-scan shows the right coronary artery aneurysm (white arrows) and its connection (black arrow) with the aorta. MPA, main pulmonary artery.

Panel C. Transesophageal echocardiography shows the enlarged orifice of right coronary artery (small arrow) and the large aneurysm (large arrow).

Panel D. Surgical views of the huge right coronary artery aneurysm (small arrows) and aorta (large arrow).

—Report on Experiments and Clinical Cases—

Significance of Plaque Disruption Sites in Acute Coronary Syndrome

Koji Seimiya, Shigenobu Inami, Masamichi Takano, Takayoshi Ohba, Shunta Sakai, Teruo Takano and Kyoichi Mizuno

Cardiovascular Center, Chiba-Hokusoh Hospital, Nippon Medical School

Abstract

Coronary plaque disruption and subsequent thrombosis occur in both unstable angina (UA) and acute myocardial infarction (AMI). However, it is unclear why UA and AMI have different clinical courses. The purpose of this angiographic study was to examine whether the longitudinal plaque disruption site is a factor that can be used to distinguish these two conditions. Seventy-two patients with AMI or UA in whom ischemia- or infarct-related arteries and plaque disruption sites could be determined were enrolled. The plaque disruption sites were classified as upstream type or downstream type. The upstream type and downstream type were defined as plaque rupture site located proximal and distal, respectively, to the maximum stenosis on angiography. The frequency of the upstream type was significantly higher in patients with AMI (60.0%) than in patients with UA (18.5%). On the other hand, the frequency of the downstream type was higher in patients with UA (81.5%) in patients with AMI (40.0%; $p<0.01$). The longitudinal plaque disruption site may thus be a factor that can be used to distinguish these two diseases.

(J Nippon Med Sch 2006; 73: 141–148)

Key words: acute coronary syndrome, myocardial infarction, unstable angina, plaque disruption

Introduction

Coronary plaque disruption followed by thrombus formation is considered an important factor in the pathogenesis of acute coronary syndrome (ACS), including acute myocardial infarction (AMI) and unstable angina (UA), and results in progression of coronary stenosis, which can be confirmed with several kinds of studies such as pathologic examination, angiography, intravascular ultrasonography, and angioscopy[1–4]. Plaque disruption occurs mainly at so-called shoulder lesions showing focal accumulation of foam cells, a thin fibrous cap, and/or a large lipid pool and high circumferential stress on the plaque[4,5].

Although the depth of plaque disruption, the condition of the thrombus, and an interruption of blood flow may help differentiate AMI from UA[3], it remains unclear why these two clinical conditions arise from similar pathological conditions. The aim of this study was to identify an additional factor that can be used to distinguish AMI from UA. The basic principle at issue in this study is that the plaque disruption site may influence the clinical presentation of ACS. There is a possibility that

Correspondence to Kyoichi Mizuno, MD, Cardiovascular Center, Chiba-Hokusoh Hospital, Nippon Medical School, 1715 Kamakari, Inba-mura, Inba-gun, Chiba 270–1694, Japan
E-mail: mizunok@nms.ac.jp
Journal Website (http://www.nms.ac.jp/jnms/)

plaque rupture at a proximal site of plaque and thrombus formation might strongly interfere with the regulation of blood flow, in comparison to a plaque rupture at a distal site. We hypothesized that thrombus accompanied by plaque rupture at a proximal site might cause total occlusion and thus result in AMI. On the other hand, thrombus accompanied by plaque rupture at a distal site might induce nontotal occlusion and result in UA. To verify this hypothesis, we investigated plaque rupture sites in patients with ACS using coronary angiography.

Methods

We evaluated 348 consecutive patients who underwent coronary angiography and were diagnosed with AMI or UA from May 1997 through March 2004 at our institution. Patients in whom ischemia- or infarct-related arteries (IRAs) and plaque rupture sites could not be determined with angiography were excluded. Finally, 72 patients in whom IRAs and plaque rupture sites could be clearly determined with angiography were enrolled. Then we evaluated the locations of plaque rupture and compared clinical characteristics and angiographic findings between AMI and UA. Informed consent was obtained from all patients enrolled in this study.

Criteria of AMI and UA

UA was defined as either an exacerbation of angina that was previously stable, such as angina occurring at rest, or the new onset of chest pain occurring at rest. The diagnosis of AMI was based on a characteristic history of prolonged chest pain, diagnostic electrocardiographic changes, an elevation in the serum creatine kinase level, the creatine kinase MB fraction ($\geq$2 times the upper limit of the normal value), and/or elevation of troponin T levels ($\geq$0.1 ng/ml).

Coronary Angiography

Coronary angiography was performed with standard procedures from the femoral or radial arteries. After 2,000 units of heparin was administered, qualifying and quantitative angiography was performed to assess lesion morphology and the severity of stenosis. Each coronary artery was closely observed with at least two projections in the right coronary artery and three projections in the left anterior descending artery and left circumflex artery. Quantitative coronary angiograms were analyzed with a computer-assisted, automated edge-detection algorithm (CMS, Medical Imaging System, Nuenen, The Netherlands) by one angiographer. The qualitative morphologic analyses of all angiograms were performed by two experienced angiographers who were blinded to clinical presentation.

Evaluation of Ischemia- or Infarct -Related Arteries and Lesions

IRAs were defined as arteries originally perfusing an area distal to the lesion on a specific coronary artery on the basis of the distribution of transient or persistent ischemic ST-T changes on 12-lead electrocardiography, transient or persistent asynergic area on two-dimensional echocardiography, left ventriculography, and scintigraphy. After the locations of IRAs were determined, ischemia- or infarct-related lesions (IRLs) could be identified. IRLs were the most severe lesions or complex lesions in the IRAs.

Evaluation of Plaque Disruption Sites

We classified the coronary angiographic morphology of AMI and UA into six categories, which included total occlusion, simple lesions (type I), and four variable degrees of luminal narrowing (types IIa, IIb, IIc, IId)[6] **(Fig. 1)**. Type I lesions represent luminal narrowing resulting from negative endoluminal images with smooth borders and broad necks. Type IIa lesions represented irregular, poorly defined, or hazy borders with sharp leading or trailing edges that either overhung or were perpendicular to the vessel walls. Type IIb lesions, including ulcerative lesions, were characterized by focal external eversion or protrusion of contrast media and diffuse luminal irregularities. Type IIc lesions included luminal narrowing with ellipsoid contrast pooling adjacent to the diseased portion, i.e., so-called extraluminal contrast pooling, and single or

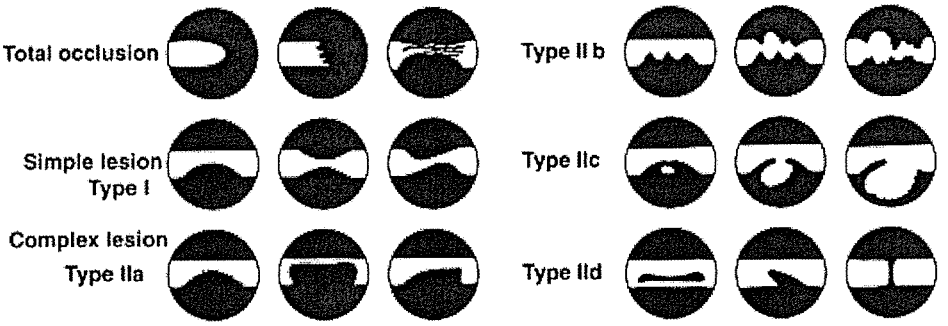

Fig. 1 Angiographical morphologies of plaque disruption site

paired short, thin, linear radiolucency with or without a variable degree of outpouching, and definite outpouching with or without radiolucency. Type IId lesions included variable forms and grades of linear or club-shaped intraluminal radiolucency caused by membranous or band-like structures. These radiolucent lesions may be parallel, spiraled, angulated, or perpendicular to the vessel wall. An angiographic plaque rupture was defined as an ulceration and an angle between the plaque shoulder and the vessel wall, for example a narrow neck.

According to the definition of IRLs, plaque rupture sites were divided into two groups, namely an upstream type and a downstream type. If the plaque rupture site was at the proximal portion of the maximum stenotic site, it was defined as an upstream type, and if the plaque rupture site was at the distal portion, it was defined as a downstream type. However, we could not determine the upstream or downstream part in cases of total occlusion, simple lesions, multiple ulcerations, or slit lesions or in cases with ulceration in the middle of stenosis.

Statistical Analysis

Data are expressed as the means ± SD. categorical variables were analyzed with the chi-square test or Fisher's exact provability test. Whether data were normally distributed or not was examined with the Kolmogrov-Sminov test. If data were normally distributed, an unpaired Student's *t*-test or Welch's *t*-test was used to compare groups. Otherwise, the Mann-Whitney U test was used. Differences were considered to be statistically significant at $p<0.05$.

Results

Plaque Disruption Site

Two hundred twenty patients, including 121 patients with simple lesions and 99 patients with total occlusion, were excluded from this study because plaque rupture sites could not be diagnosed. Forty-seven patients with complex lesions were also excluded because the upstream or downstream part of the plaque rupture could not be determined. Nine patients with small or thin anatomic coronary structures could not be evaluated with the coronary angiography equipment. Finally, 72 patients in whom the upstream or downstream plaque rupture sites could be clearly identified were included in this study.

Of the 72 patients with clearly identified plaque rupture sites, 45 had AMI and 27 had UA. In the AMI group, 27 sites were categorized upstream type and 18 as downstream. In the UA group, 5 sites were categorized as upstream and 22 as downstream. The frequency of upstream sites was significantly higher in patients with AMI than in those with UA. On the other hand, the frequency of downstream sites was higher in patients with UA than in those with AMI. Between the AMI group and the UA group, there were no significant differences in percent diameter stenosis, minimum lumen diameter, or lesion length (**Table 1**).

Cases of the upstream type and downstream types are shown in **Figure 2, 3**, respectively.

Baseline and Angiographic Characteristics

The baseline and angiographic characteristics of

Table 1 Lesion Characteristics on Angiogram

	Acute Myocardial Infarction n=45	Unstable Angina n=27	*P*
Disruption Site			
Upstream	27 (60.0)	5 (18.5)	<0.05
Downstream	18 (40.0)	22 (81.5)	
QCA Analysis			
Percent Diameter Stenosis, %	88±13	89±11	0.76
Minimal Lumen Diameter, mm	0.98±0.55	0.96±0.26	0.72
Lesion Length, mm	6.77±2.64	8.24±1.40	0.15

Values are n (%) or the mean±SD. QCA indicates quantitative coronary angiography.

Fig. 2 Plaque disruption at upstream site in patient with AMI

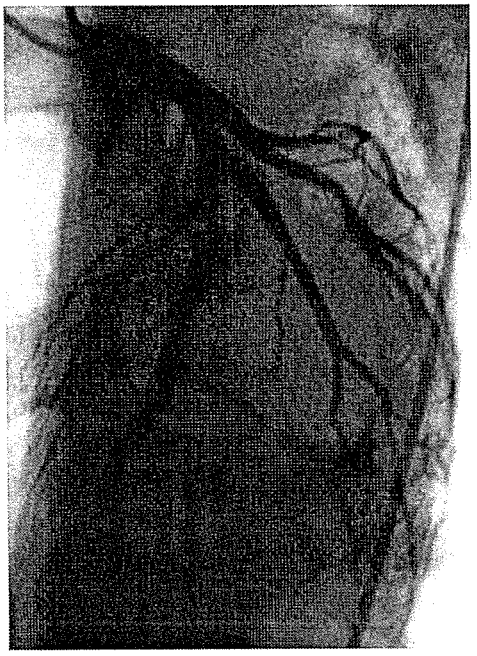

Fig. 3 Plaque disruption at downstream in patient with UA

the AMI group and the UA group are summarized in **Table 2**. There were no significant differences in age, gender, body mass index, plasma lipid levels, or the frequencies of diabetes mellitus, hypertension, or smoking habit. In addition, no significant differences were observed in the location of culprit coronary arteries or the number of diseased vessels.

Angiographic Morphology of Plaque Disruption Sites

There were no significant differences in the angiographic morphology of plaque rupture sites between the AMI and UA groups. However, type IIa lesions, which demonstrated irregular, poorly defined, or hazy borders with sharp leading or trailing edges that hung over the vessel walls, were a major morphological finding in each group. A type IIc lesion was observed in only one patient with UA, whereas type IId lesions were observed in 6 patients with AMI and in 9 patients with UA (**Table 3**).

Differentiation of Plaque Disruption Sites in Patients with AMI

The AMI group included 34 patients with ST elevation myocardial infarction and 11 patients with non-ST elevation myocardial infarction. There were no significant differences in plaque rupture sites between the groups (**Table 4**). There were no significant differences in other baseline characteristics between the groups.

Discussion

To the best of our knowledge, this is the first study to find that AMI arises from a plaque

Table 2 Baseline Characteristics

	Acute Myocardial Infarction n = 45	Unstable Angina n = 27	*P*
Age, yr	65.1 ± 10.4	62.6 ± 9.7	0.37
Male, Female	31 (68.8)	17 (65.9)	0.39
Diabetes Mellitus	15 (33.3)	6 (22.2)	0.23
Hypertension	22 (51.1)	14 (51.8)	0.49
Hyperlipidemia	23 (53.1)	13 (48.1)	0.49
Serum Lipid Levels			
Total Cholesterol, mg/dl	200.3 ± 36.7	185.1 ± 31.7	0.13
Triglycerides, mg/dl	147.3 ± 138.0	117.6 ± 58.1	0.33
High-density Lipoprotein Cholesterol, mg/dl	43.8 ± 12.7	43.8 ± 12.7	0.28
Smoking History	33 (75.0)	16 (59.2)	0.16
Body Mass Index, Kg/mm^2	23.7 ± 2.8	24.9 ± 4.0	0.19
Distribution of Culprit Lesions			
Right Coronary Artery	10 (22.2)	10 (37.0)	0.38
Left Descending Artery	21 (46.6)	11 (40.7)	
Left Circumflex Artery	14 (31.1)	6 (22.2)	
Number of Diseased Vessel			
1 Vessel	23 (51.1)	11 (40.7)	0.42
2 Vessels	17 (37.7)	10 (37.7)	
3 Vessels	5 (11.1)	6 (22.2)	

Values are n (%) or the mean ± SD.

Table 3 Angiographic Morphology of the Plaque Disruption Site

	Acute Myocardial Infarction n=32	Unstable Angina n=23	*P*
IIa	28	15	0.11
IIc	0	1	
IId	4	7	

Values are n (%) or the mean ± SD.

Table 4 Differentiation of the Plaque Disruption Site in patients with MI

	ST elevation MI n=34	Non-ST elevation MI n=11	*P*
Upstream	21	6	0.73
Downstream	13	5	

Values are n (%). MI indicates myocardial infarction

disruption of the upstream part and that UA arises from a plaque disruption of the downstream part in most cases. A disruption of the vulnerable plaque exposes the thrombogenic contents of an atheroma to flowing coronary blood and initiates thrombus formation, which may lead to either a blood-flow limitation or total occlusion[37]. The degree of flow interruption is influenced by several factors, such as the magnitude of plaque rupture, the severity of pre-existing coronary stenosis, the amount of thrombus adhering to the plaque rupture site, the lability of the thrombus, the balance of coagulability, and the severity of coronary spasm. All these factors may influence on the clinical setting of AMI and UA.

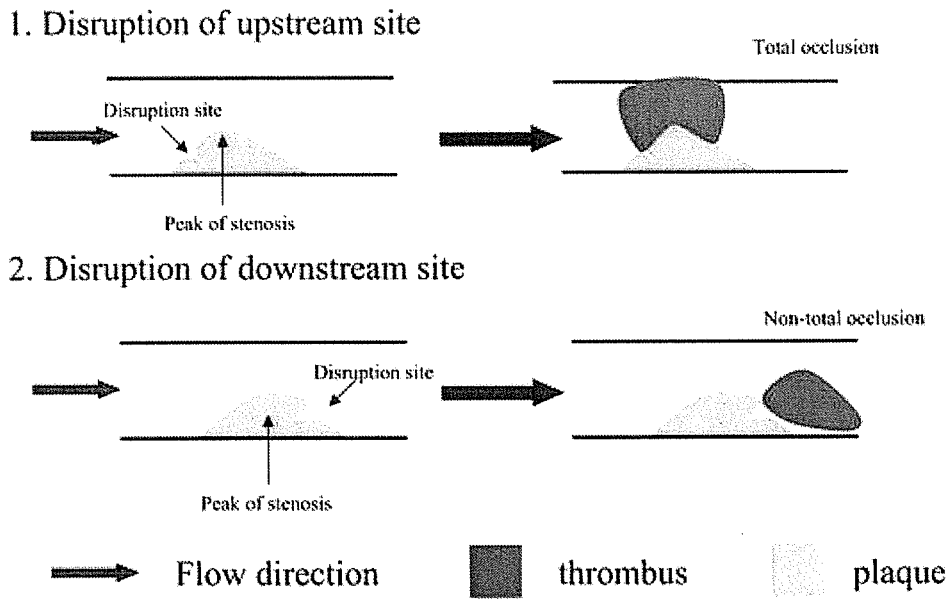

Fig. 4 Relation between the Plaque Disruption Site and Flow Interruption

Previous Mechanisms to Differentiate AMI and UA

A disruption of the atheromatous plaque following thrombus formation is believed to be the initial step in the onset of ACS. Fuster et al. have proposed the following explanation for differences between AMI and UA[3,8]. In UA with progressive symptoms, but without chest pain at rest, a plaque rupture with a change in the geometric configuration of the plaque, but without any overlying thrombus, can increase the severity of pre-existing stenosis. However, in the case of UA with chest pain at rest, the plaque rupture and pre-existing stenosis are both less severe, and, therefore, thrombosis is transient or labile. An incomplete interruption of blood flow leads to UA. In AMI, the plaque disruption is deeper than in UA, and the thrombus, which is anchored to a large rupture site, is more firmly fixed. The duration of coronary artery occlusion in AMI is also longer than in UA[9].

In terms of an interruption of blood flow, our previous angioscopic study revealed occluded red thrombi, which are formed by blood stasis, in patients with AMI. On the other hand, nonoccluded white thrombi, which are formed through incomplete interruption of blood flow, were observed in patients with UA[10]. In addition to the severity of blood flow limitation, other mechanisms that might be used to distinguish AMI from UA are vessel wall injury and hypercoagulability[11,12].

Plaque Disruption Sites

Plaque disruption often occurs on a thin fibrous cap that is composed of abundant inflammatory cells and scant smooth muscle cells (SMCs). Recently, Dirksen et al. investigated the relationship between blood-flow direction and the cellular composition of carotid plaques in a consecutive autopsy series of 45 patients. They found that the upstream shoulder of plaques tended to contain more macrophages than did the downstream shoulder. They also found that many rupture sites were located in the upstream part of the plaque[13]. Experimental studies have shown that high shear stress increases expression of endothelial adhesion molecules, such as intercellular adhesion molecule and vascular cell adhesion molecule, thus resulting in enhanced leukocyte adherence[14,15]. The upstream shoulder is exposed to high shear stress, which activates endothelium-derived nitric oxide (NO) synthesis and NO production. This chronically enhanced NO production inhibits SMC protein synthesis and SMC proliferation[16,17]. Conversely, the downstream shoulder part of the plaque, which has a relatively

low shear stress, shows larger SMC-rich areas than does the upstream part. Since the upstream shoulder of the plaque contains many inflammatory cells and few SMCs, it is more fragile than the downstream shoulder, which contains many SMCs.

Mechanical stress might also influence the development of plaque rupture. Richardson et al. investigated plaque disruption sites in autopsy cases. In cases with extracellular lipid pools in the intima, many plaque disruptions occurred at the junction of the plaque cap and the center of the plaque cap. The differentiation of the plaque disruption site was influenced by the degree of circumferential stress and shear force in the arterial wall and by the presence of a calcified plate within the intima[5]. From the viewpoint of mechanical stress, the downstream plaque shoulders could rupture more easily owing to the effects of such stress.

If the maximum stenotic site is located distal to plaque disruption, then the part of the disrupted plaque with thrombus may cause either severe stenosis or occlusion in the artery. This condition may lead to AMI. On the other hand, if maximum stenosis site is proximal to plaque disruption, then plaque disruption followed by thrombus might not induce total occlusion (**Fig. 4**). This study thus suggests that the plaque rupture site might be an important factor for distinguishing UA and AMI.

Study Limitations

We excluded totally occluded lesions and very small arteries on angiograms, because their rupture sites were unclear. In this study, the plaque ruptures in 119 of 348 patients (34.1%) and plaque rupture sites in 72 of 348 patients (20.6%) were clearly detected by angiograms. Rioufol et al. could identify plaque ruptures in 9 of 24 (37.5%) patients with ACS using intravascular ultrasound[18]. It is difficult to identify plaque disruption sites with angiography, as with other modalities, because of superimposed thrombi. The findings of Rioufol et al. are consistent with the small percentage of patients in whom plaque rupture sites could be accurately determined in our study.

Conclusions

The frequency of upstream disruption was higher in patients with AMI, whereas the frequency of downstream disruption was higher in patients with UA. This angiographic study showed that plaque disruption site might be used to distinguish UA and AMI.

References

1. Mizuno K, Miyamoto A, Satomura K, et al.: Angioscopic coronary macromorphology in patients with acute coronary disorders. Lancet 1991; 6: 809–812.
2. Falk E, Shah PK, Fuster V: Coronary plaque disruption. Circulation 1995; 92: 657–671.
3. Fuster V, Badimon L, Badimon J, Chesebro J: The pathogenesis of coronary artery disease and acute coronary syndrome. N Eng J Med 1992; 326: 310–318.
4. Libby P: Molecular bases of the acute coronary syndrome. Circulation 1995; 91: 2844–2850.
5. Richardson PD, Davies MJ, Born GVR: Influence of plaque configuration and stress distribution on fissuring of coronary atherosclerotic plaques. Lancet 1989; 21: 941–944.
6. Nagoshi T, Koiwaya Y, Doi H, Eto T: Angiographic coronary morphology in patients with ischemic heart disease. J Cardiol 2000; 36: 91–102.
7. Daves MJ, Thomas AC: Plaque fissuring: the cause of acute myocardial infarction, sudden ischemic death, and crescendo angina. Br Heart J 1985; 53: 363–373.
8. Fuster V, Badimon L, Badimon J, Chesebro J: The pathogenesis of coronary artery disease and acute coronary syndrome. N Eng J Med 1992; 326: 242–250.
9. Zaacks SM, Liebson PR, Calvin JE, Parrillo JE, Klein LW: Unstable angina and non-Q wave myocardial infarction: Dose the Clinical Diagnosis Have Therapeutic Implications? J Am Coll Cardiol 1999; 33: 107–118.
10. Mizuno K, Satomura K, Miyamoto A, et al.: Angioscopic evaluation of coronary-artery thrombi in acute coronary syndromes. N Eng J Med 1992; 326: 287–291.
11. Gimbrone MA Jr, Cybulsky MI, Kume N, Collins T, Resnick N: Vascular endothelium: an integrator of pathophysiological stimuli in atherogenesis. Ann NY Acad Sci 1995; 748: 122–132.
12. Ambrose JA: Plaque disruption and the acute coronary syndrome of unstable angina and myocardial infarction: If the substrate is similar, why is the clinical presentation different? J Am Coll Cardiol 1992; 19: 1653–1658.
13. Dirksen MT, Van der Wal AC, Van den Berg FM, Van der Loos CM, Becker AE: Distribution of inflammatory cells atherosclerotic plaque relates to the direction of flow. Circulation 1998; 98: 2000–2003.
14. Walpola PL, Gotlieb AI, Cybulsky MI, Langille BL:

Expression of ICAM-1 and VCAM-1 and monocyte adherence in arteries exposed to altered shear stress. Arterioscler Thromb Vasc Biol 1995; 15: 2–10.
15. Tropea BI, Huie P, Cooke JP, et al.: Hypertension-enhanced monocyte adhesion in experimental atherosclerosis. J Vasc Surg 1996; 23: 596–605.
16. Kolpakov V, Gordon D, Kulik TJ: Nitric oxide-generating compounds inhibit total protein and collagen synthesis in cultured vascular smooth muscle cells. Circ Res 1995; 76: 305–309.
17. Garg UC, Hassid A: Nitric oxide-generating vasodilators and 8-bromo-cyclic GMP inhibit mitogenesis and proliferation of cultured rat vascular smooth muscle cells. J Clin Invest 1989; 83: 1774–1777.
18. Rioufol G, Finet G, Ginon I, et al.: Multiple atherosclerotic plaque rupture in acute coronary syndrome. Circulation 2002; 106: 804–808.

(Received, February 23, 2006)
(Accepted, April 10, 2006)

Stent-Based Delivery of Antisense Oligodeoxynucleotides Targeted to the PDGF A-Chain Decreases In-Stent Restenosis of the Coronary Artery

Yuxin Li, MD, PhD, Noboru Fukuda, MD,† Satoshi Kunimoto, MD,* Shin-ichiro Yokoyama, MD,* Kazuhiro Hagikura, MD,* Taro Kawano, MD,* Tadateru Takayama, MD,* Junko Honye, MD,* Naohiko Kobayashi, MD,‡ Hideo Mugishima, MD,§ Satoshi Saito, MD,* and Kazuo Serie¶*

Background: Although the use of drug-eluting stents (DESs) has been shown to limit neointima hyperplasia, currently available DESs may adversely affect reendothelialization, possibly precipitating cardiac events. We evaluated the effect of an antisense oligodeoxynucleotide (ODN) targeted to the platelet-derived growth factor (PDGF) A-chain on in-stent restenosis in pig coronary artery.

Methods: A bare metal stent coated with phosphorothioate-linked antisense ODN or nonsense ODN, or a bare metal stent without ODN (control), was implanted in the mid segment of the left anterior descending artery (LAD). Twenty-eight days after implantation, angiography and intravascular ultrasound (IVUS) were performed, the LAD was removed, and stenosis was evaluated pathologically.

Results: Volumetric stenosis ratios were 64 ± 11.9, 44 ± 3.4, and 26 ± 3.8% in coronary arteries implanted with control, nonsense ODN-coated, and antisense ODN-coated stents, respectively. In angioscopic findings, the lumen surface was smooth in the stented segments in all groups. Struts of antisense ODN-coated stents were observed embedded in the neointima, whereas embedding was not observed in nonsense ODN-coated stents or control stents, indicating a decrease in hyperplasia in response to antisense ODN treatment. Pathologic findings showed 77 ± 5.8, 68 ± 12.2, and 38 ± 5.3% stenosis in coronary arteries implanted with control stents, nonsense ODN-coated stents, and antisense ODN-coated stents, respectively. A continuous lining of endothelial cells was observed along the lumen of coronary arteries implanted with antisense ODN-coated stents.

Conclusions: Stent-based delivery of an antisense ODN targeted to the PDGF A-chain effectively inhibits neointima formation after stent implantation in pig coronary artery by suppressing VSMC hyperplasia and preserving endothelialization. Antisense-ODNs may provide a therapy for in-stent restenosis of the coronary artery.

Key Words: restenosis, antisense oligonucleotides, PDGF A-chain, endothelialization

(*J Cardiovasc Pharmacol*™ 2006;48:184–190)

INTRODUCTION

Despite the widespread use of intracoronary stents, in-stent restenosis remains a major clinical problem. Neointima formation with vascular smooth muscle cell (VSMC) hyperplasia is believed to play a critical role in in-stent restenosis.[1] Drug-eluting stents (DESs) have been shown to be effective to prevent in-stent restenosis. DESs with sirolimus or paclitaxel have been used widely to prevent in-stent restenosis in humans.[2–5] Sirolimus halts cell-cycle progression,[6] and sirolimus-coated DESs can prevent in-stent restenosis by inducing complete inhibition of VSMC hyperplasia. However, complications such as subacute thrombosis or late thrombosis have been reported in patients implanted with a sirolimus-coated DES.[7,8] Sirolimus prevents reendothelialization of the inner side of the metal stent, which may cause late thrombosis. These complications have led to the development of second-generation DESs that do not induce late thrombosis.

Platelet-derived growth factor (PDGF), a potent stimulator of VSMC proliferation, is a dimer composed of a disulfide-linked polypeptides A-chain and B-chain.[9,10] There are 3 isoforms of PDGF (AA, AB, and BB). Nilsson et al[11] showed that normal growth-arrested VSMCs do not express PDGF messenger ribonucleic acid (mRNA), whereas cultured VSMCs and VSMCs in atherosclerotic plaques express PDGF A-chain mRNA and secrete PDGF-AA protein. We have reported that spontaneously hypertensive rat–derived VSMCs, which show exaggerated proliferation and the synthetic phenotype, express increased levels of PDGF A-chain mRNA.

Antisense oligodeoxynucleotides (ODNs) have been used clinically to suppress gene expression. Antisense ODNs can be used to inhibit DNA transcription and the production of mature mRNA and to inhibit peptide synthesis. Antisense therapy is being developed for the treatment of in-stent restenosis. We have shown that an antisense ODN to the PDGF A-chain inhibits the exaggerated proliferation of VSMCs from spontaneously hypertensive rats.[12–14] In a rat model of

From the *Department of Medicine, Division of Cardiovascular Medicine, Nihon University School of Medicine, Tokyo, Japan; †Advanced Research Institute for the Sciences and Humanities, Nihon University, Tokyo, Japan; ‡Department of Hypertension and Cardiorenal Medicine, Dokkyo University School of Medicine, Tochigi, Japan; §Department of Advanced Medicine, Division of Cell Regeneration and Transplantation, Nihon University School of Medicine, Tokyo, Japan; and ¶Gentier Biosystems Incorporation, Tokyo, Japan.

Reprints: Dr Noboru Fukuda, Advanced Research Institute for the Sciences and Humanities, Nihon University, 30-1 Oyaguchi-Kamimachi Itabashi-ku, Tokyo 173-8610, Japan (e-mail: fukudan@med.nihon-u.ac.jp).

neointima formation in the carotid artery after balloon injury, we showed a 60% decrease in neointima in response to antisense therapy.

To aid in the development of safer DESs that do not inhibit reendothelialization, we examined the effects of stent-based delivery of an antisense ODN targeted to the PDGF A-chain on in-stent restenosis and reendothelialization of the coronary artery in pigs.

METHODS

Synthetic Antisense Oligodeoxynucleotides to the Platelet-Derived Growth Factor (A-chain)

We used a 15-mer antisense ODN to the PDGF A-chain (5′-AGGTCCTCATCGCGT-3′) complementary to the region containing the initiation codon of human and rat PDGF A-chain complementary deoxyribonucleic acid (cDNA), as reported previously.[12] A nonsense control ODN (5′-TGCCGT-CAGCTGCTA-3′) contained an identical proportion of bases but in random order. ODNs were synthesized with a DNA synthesizer (model 394; Applied Biosystems, Foster City, CA, USA) and purified on an OPC column (Applied Biosystems). ODNs were modified with a phosphorothioate linkage by oxidizing phosphate linkages with 3H-1,2-benzodithiol-3-one-1,1-dioxide instead of the standard iodine reagent.[15]

Animal Preparation and Stent Implantation

Animal care and handling were performed in accordance with the National Institutes of Health Guide for the Care and Use of Laboratory Animals and were approved by the Institutional Animal Care and Use Committee of Nihon University. Eighteen domestic male pigs weighing 22–28 kg each were used in the present study. Bare metal stents (n = 6), nonsense ODN-coated stents (n = 3), and antisense ODN-coated stents (n = 9) were implanted into the left anterior descending artery. Hydrogel-coated matrical stents (diameter 3.5 mm, length 20 mm, Interventional Radiology Co., Ltd., Tokyo, Japan) were dip-coated in 20 μg/mL antisense or nonsense ODN solution containing 100 μ/mL polyethylenimine reagent (MBI Fermentas) for 10 min and were air-dried for 10 min. Control stents were treated identically but were not coated with ODN.[16,17]

Aspirin (325 mg) was administered 1 day before stent implantation. After overnight fasting, intramuscular injection of 25 mg/kg sodium pentobarbital was administered and anesthesia was maintained with a continuous intravenous infusion of 1 mg/kg per hour ketamine chloride. A 5000-IU bolus of heparin was administered intravenously. After endotracheal intubation, controlled mechanical ventilation was established at a tidal volume of 10–15 mL/kg with a volume-cycle ventilator (Servo 900-E; Siemens-Elema Inc, Stockholm, Sweden).

Continuous hemodynamic and surface electrocardiography monitoring were maintained throughout the procedure. The right carotid artery was inserted with a 6F sheath. After baseline coronary angiography, mechanical intravascular ultrasound (IVUS) (40 MHz, Atlantis™; Boston Scientific Corp., Natick, MA, USA) of the left anterior descending artery was performed. IVUS catheters were automatically pulled back at 0.5 mm per second. IVUS images were recorded continuously on Super VHS videotape for analysis. Based on the IVUS images, a segment of diameter of 3.0 mm in diameter was selected for stent implantation. Stents of 3.5 mm × 20 mm were used with a 12-atm inflation pressure to reach a 1.3:1 stent-to-artery ratio. Immediately after implantation, IVUS was performed to confirm the stent-to-artery ratio. If the ratio was not adequate, the stent balloon was reinflated with higher pressure in the stented segment. Follow-up coronary angiography and IVUS were performed 28 days after implantation, and the stented coronary arteries were harvested for angioscopic evaluation and pathologic analysis.

To assess the distribution of antisense ODN targeted to the PDGF A-chain, stents coated with fluorescein-isothiocyanate (FITC)-labeled antisense ODN were implanted. Twenty-four hours after implantation, the heart was removed, and the stented coronary artery segment was harvested and fixed in 4% paraformaldehyde. Sections were examined by fluorescence microscopy. In addition, 3.5 mm × 23 mm sirolimus-coated stents (Cypher™; Cordis Corp., Miami Lakes, FL, USA) were implanted by the same method. After 28 days, the stented coronary artery segment was harvested for angioscopic evaluation and pathologic analysis.

Intravascular Ultrasound Measurements

Follow-up IVUS images were recorded on Super VHS tape and analyzed with a computer-based contour detection program for 3-dimensional reconstruction and volumetric measurement (NetraIVUS™ software package for Windows NT®, ScImage Corp, Los Altos, CA, USA). Cross grids recorded on the IVUS images were used for calibration. The interface between the neointima and lumen and the outer border of the external elastic membrane were traced manually. On the basis of the manual traces, the computer software determined measurements for lumen volume (LV) and vessel volume (VV). Volumetric in-stent restenosis (%AS) was calculated as (VV-LV)/VV.

Angioscopic Evaluations

Twenty-eight days after stent implantation, the stented segment of coronary artery was harvested after perfusion with saline at physiologic pressure. Angioscopic observations were made while the blood was perfused away. We used an MC-800E angioscope (Nihon Kohden, Tokyo, Japan) and an AS-003 optic fiber (Nihon Kohden). We examined the entire stented segment from the distal to the proximal end and evaluated the inner surface for neointima and thrombi.

Pathologic Analysis

Three cross sections were cut for pathologic analysis, 1 each from the proximal, central, and distal portions along each stent. Sections were ground to a thickness of approximately 50 μm and stained with hematoxylin and eosin. A computerized imaging system (ImageJ 1.30, NIH) was used for histomorphometric measurements of the following parameters: lumen area, defined as the area circumscribed by the neointima–lumen border, and neointima area, defined as the area between the lumen and the internal elastic lamina (IEL). In-stent restenosis was estimated as the neointima area/IEL area.

Statistical Analysis

Data are expressed as mean ± SEM. Mean values of variables were compared by a 2-sided unpaired *t*-test. A value of $P < 0.05$ was considered statistically significant.

RESULTS

Distribution of Antisense Oligodeoxynucleotide Targeted to the PDGF A-Chain

The distribution of FITC-labeled antisense ODN 24 hours after implantation is shown in Figure 1. FITC-labeled antisense ODN was distributed predominantly in the endothelial layer of the stented coronary artery.

IVUS Findings of In-Stent Restenosis

The stent/artery ratio was 1.3 ± 0.1, 1.3 ± 0.1, and 1.4 ± 0.1 in coronary arteries implanted with bare metal stents, nonsense ODN-coated stents, and antisense ODN-coated stents, respectively. There were no significant differences between the 3 groups.

Occlusive neointima filled the lumen and encircled the ultrasound catheter in arteries implanted with control stents (Fig. 2A, B), whereas the lumen was clear in coronary arteries implanted with antisense ODN-coated stents (Fig. 2C, D). Volumetric in-stent restenosis ratios were 64 ± 11.9, 44 ± 3.4, and 26 ± 3.8% in coronary arteries implanted with bare metal stents, nonsense ODN-coated stents, and antisense ODN-coated stents, respectively. The in-stent restenosis ratio was significantly less in the antisense group than in the control and nonsense groups (Fig. 2E).

Angioscopic Findings

The lumen surface was smooth and lacked protrusions in the stented segments of coronary arteries in all groups (Fig. 3A–C). Struts in the antisense ODN-coated stent group were visibly embedded in the neointima (Fig. 3C), whereas embedding was invisible in the nonsense ODN-coated stent and control stent groups, indicating decreased neointimal hyperplasia in the antisense group. An irregular surface with protrusions into the lumen were observed in sirolimus-coated stented segments, and some ragged red thrombi were observed adhering to the lumen surface (Fig. 3D).

Pathologic Findings

Microscopic images obtained 28 days after implantations are shown in Figure 4. Neointima formation was less in coronary arteries implanted with antisense ODN-coated stents than in arteries implanted with control stents or nonsense ODN-coated stents. In-stent stenosis in distal, central, and proximal areas of stented artery are shown in Figure 5. In-stent stenosis of control, antisense, and nonsense groups was 70 ± 9.7, 58 ± 4.2, and 41 ± 5.5% in the proximal end; 77 ± 5.8, 68 ± 12.2, and 38 ± 5.3% in the central segment; and 65 ± 9.1, 70 ± 4.9, and 38 ± 5.9% in the distal end. These findings indicate that the antisense ODN targeted to the PDGF A-chain significantly inhibited in-stent neointima formation.

Differences in endothelialization differed between sirolimus-coated stents and antisense ODN-coated stents (Fig. 6). Patchy and interrupted endothelial cells in the artery lumen were observed in arteries implanted with sirolimus-coated stents (Fig. 6A), whereas a continuous lining of endothelial cells was observed in arteries implanted with antisense ODN-coated stents (Fig. 6B). There is no difference in appearance of reendothelialization among antisense ODN-coated stent, nonsense ODN-coated stent, and bare metal stent. These data suggest that the antisense ODN does not interfere with in-stent endothelialization.

DISCUSSION

Various classes of agents are available and are under investigation for the use of DESs to prevent in-stent restenosis of the coronary artery and include immunosuppressive (sirolimus), antiinflammatory (corticoid and tranilast), antiproliferative (paclitaxel, angiopeptin, and actinomycin), and antithrombotic agents (hirudin and iloprost).[18] Sirolimus halts cell-cycle progression at the G1 phase, resulting in inhibition of replication and proliferation.[6] Sirolimus halts the cell cycle nonspecifically; therefore, sirolimus-coated DESs prevent not only VSMC hyperplasia but also endothelialization, which is required for the prevention of thrombosis. Patients implanted with a sirolimus-coated DES require the administration of antiplatelet agents for at least 3 months after stent implantation.

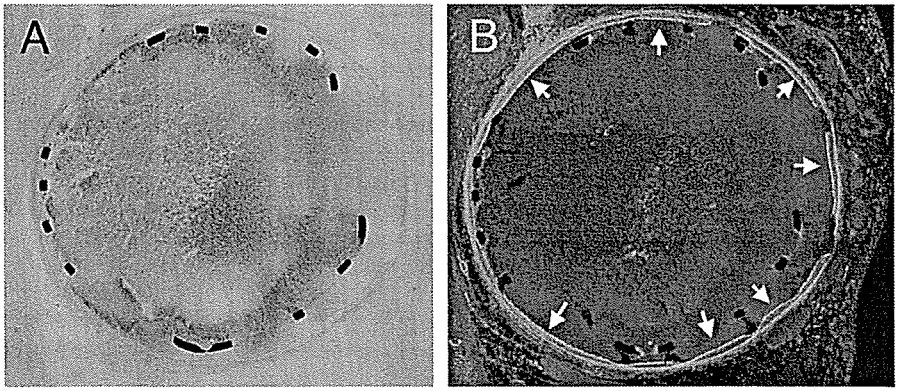

FIGURE 1. Distribution of FITC-labeled antisense ODN targeted to the PDGF A-chain in a stent 24 hours after implantation in a pig coronary artery. A. Optical microscopy. B, Fluorescence microscopy. Arrows in (B) indicate areas of ODN fluorescence.

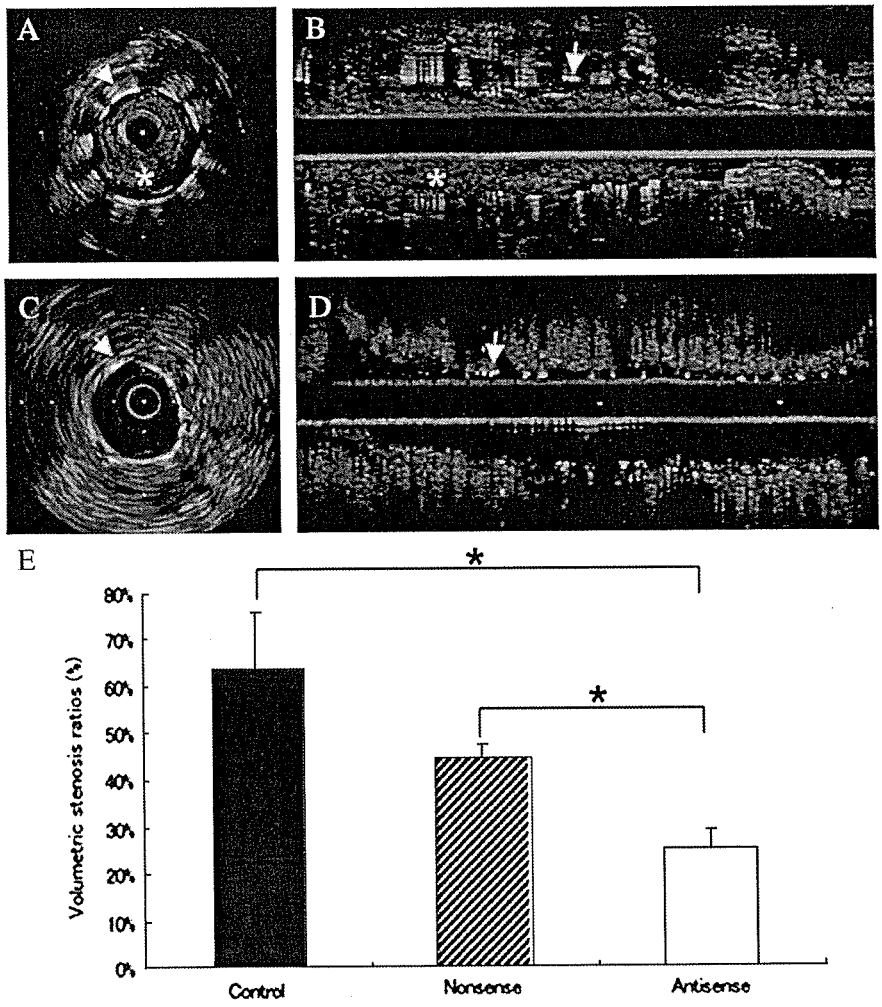

FIGURE 2. Representative cross sections (A, C) and long-axis images (B, D) of coronary arteries implanted with bare metal stents (A, B) or with antisense ODN-coated stents (C, D) assessed by intravascular ultrasound 28 days after implantation. Arrows indicate stent struts. Stars indicate neointima. E, Volumetric stenosis ratios for antisense-coated, nonsense-coated, and control stents. Data are the mean ± SEM. $*P < 0.05$.

The timing of reendothelialization differs between patients, and late thrombosis is a major problem in patients implanted with sirolimus-coated DESs. Thus, development of DESs that preserve endothelialization is necessary.

In the present study, stent-based delivery of an antisense ODN targeted to the PDGF A-chain showed a potent inhibitory effect on VSMC proliferation, showing a 60% decrease in percent volume stenosis and preservation of endothelialization. DESs with sirolimus did not preserve endothelialization.

In 2001 it was that VSMCs in the neointima originate from circulating bone marrow cells in addition to media VSMCs.[19] Intimal VSMCs, which show the synthetic phenotype, abundantly express several cytokines and growth factors, including PDGF, transforming growth factor-beta, basic fibroblast growth factor, endothelin, and angiotensin II, which are involved in neointima formation.[20] Neointima are composed of VSMCs and extracellular matrix.[21] It is likely that antisense ODN targeted to the PDGF A-chain inhibits neointima formation at least in part.

The PDGF A-chain contributes to VSMC proliferation in arterial proliferative disease. The PDGF B-chain is expressed constitutively in the vasculature and in platelets, whereas the PDGF A-chain is produced only in VSMCs of the synthetic phenotype. Kruppel-like zinc-finger transcription factor 5 (KLF5) has been established as a transcription factor that alters VSMCs from the contractile to the synthetic phenotype, inducing expression of the PDGF A-chain.[22] These findings suggest that the PDGF A-chain is a critical target for the inhibition of VSMC hyperplasia in neointima. Our results suggest that the antisense ODN targeted to the PDGF A-chain is a specific inhibitor of neointimal VSMC proliferation that does not affect endothelialization. Stent-based delivery of this antisense ODN inhibited neointima formation and preserved endothelialization in the absence of antiplatelet agents.

One problem of exogenously administered nucleic acid–based medicines, including antisense DNA, is that they are readily degraded by nucleases in vivo. However, locally delivered nucleic acids from a DES show less degradation than do systemically administered nuclei acids. In the present experiments, we chemically modified antisense ODN to the phosphorothioate type, dissolved it in hydrogel, and applied it to both the balloon and the stent, resulting in efficient delivery of

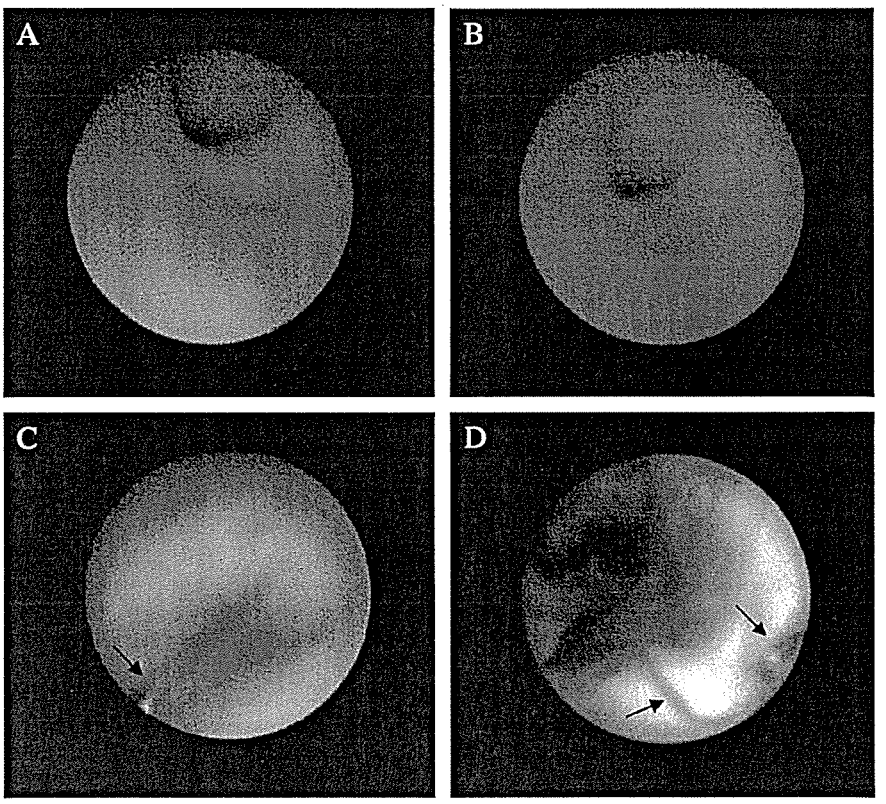

FIGURE 3. Representative angioscopic findings of stented segments of pig coronary artery implanted with bare metal stents (A), nonsense ODN-coated stents (B), antisense ODN-coated stents (C), or sirolimus-coated stents (D). Arrows indicate embedding in the neointima.

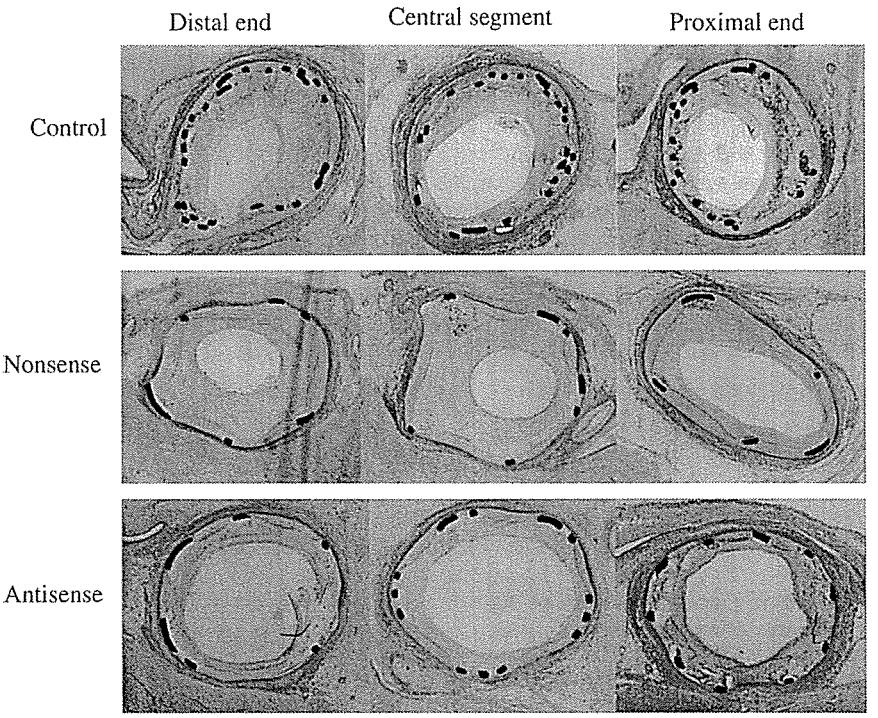

FIGURE 4. Microscopic images of pig coronary arteries implanted with bare metal stents (control), nonsense ODN-coated stents, or antisense ODN-coated stents 28 days after implantation. Sections were stained with hematoxylin and eosin.

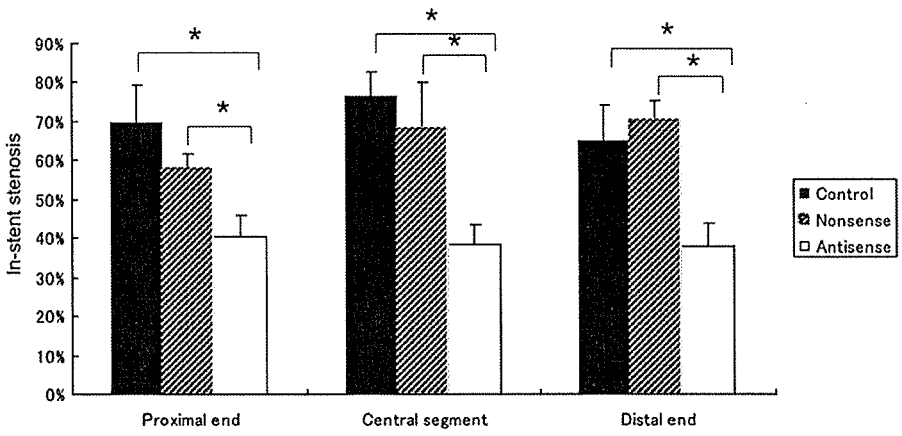

FIGURE 5. Quantification of in-stent stenosis from the microscopic images of pig coronary arteries implanted with bare metal stents (control), nonsense ODN-coated stents, or antisense ODN-coated stents 28 days after implantation. A computerized imaging system (ImageJ 1.30) was used for histomorphometric measurement of the following parameters: lumen area, defined as the area circumscribed by the neointima-lumen border, and the neointima area, defined as the area between the lumen and the internal elastic lamina (IEL). Percent in-stent restenosis was calculated as neointima area/IEL area. Data are mean ± SEM. $*P < 0.05$.

antisense ODN to the coronary artery. Nonsense ODN with a random sequence also showed a tendency to inhibit the neointima formation to a lesser extent. Similar nonspecific effects of ODN have confounded the interpretation of previous antisense studies. Several studies report that charged ODN behaves like polyanions such as heparin and heparan, which bind and sequester heparin-binding growth factors, such as basic fibroblast growth factor or PDGF, at the basement membrane.[23] Another report described the nonspecific cellular activation of the transcription factor Sp1 by phosphorothioate-linked ODN.[24]

Recent applications of antisense ODN targeted to c-myc have been reported for the prevention of in-stent stenosis of the coronary artery in pigs[25] and humans.[26] An advanced antisense ODN (AVI-4126) to c-myc–eluting stent inhibited c-myc expression and significantly inhibited neointimal hyperplasia by 40% in a pig model. C-myc is also required in the progression of cell cycle. Therefore, a DES with antisense ODN targeted to c-myc may inhibit reendothelialization in a manner similar to a sirolimus-coated DES.

There are some limitations in the present study. An important point in this animal model is that the arteries are devoid of atherosclerotic lesions, whereas in patients, most stent struts are in contact with atheromatous plaque and not with the media. In the present study, degree of in-stent restenosis was examined only at 1 month after stent implantation; longer follow-up should be performed in future experiments. The coating system in the present study is hydrogel, which is different with sirolimus-coated stents (Cypher stent). The impaired reendothelialization with the Cypher stent might be mainly related to the polymer-coated stent surface and not to the drug.[27]

Based on the results in the present study, we plan to repeat the experiments with longer follow-up and repeat the experiments in an animal model of coronary atherosclerosis. After animal experiments, we plan to apply stents coated with antisense ODN targeted to the PDGF A-chain for treatment of human coronary diseases. Clinical trials of antisense therapies have been performed for human diseases including cancer.[28,29] Even high doses of infused antisense ODN for long periods show little or no side effects or toxicity in clinical trials, indicating the safety of antisense therapy in humans. Although antisense ODNs can be applied to DESs, certain technical problems need to be addressed. In the present study, we used polyethylenimine as the delivery regent. Procedures providing more effective and safer delivery of antisense ODN from DESs should be assessed.

In the present study, we applied hydrogel to the balloon and the stent. This was particularly helpful for coating the stent with antisense ODN. We are developing a coated stent that more effectively absorbs and delivers agents to the coronary artery. At physiologic pH, antisense ODNs are negatively charged. Thus, the metal surface of the stent can be coated with a positively charged substance, enabling antisense ODNs to adhere strongly to the stent.

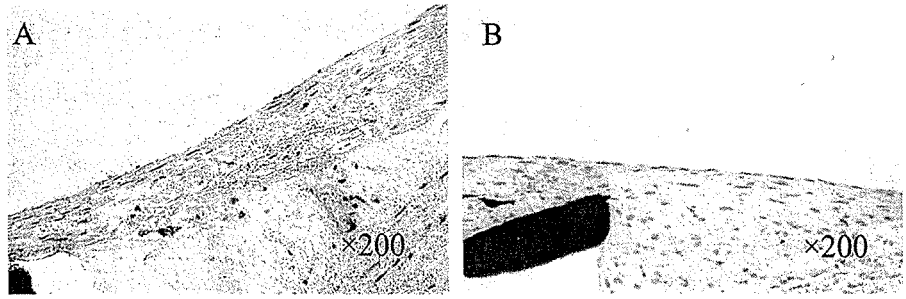

FIGURE 6. Endothelialization of pig coronary arteries implanted with antisense ODN-coated stents (A) or sirolimus-coated stents (B). Sections were stained with hematoxylin.